Technical Paper

ISSN 1997-1400 Int. J. Pavement Res. Technol. 3(6):326-335

Nondestructive Evaluation of Thickness and Bearing Capacity of Roadway Pavement Structure

Long-Sheng Huang[1+] and Yumin Vincent Kang[2]

Abstract: Field studies using the ground penetrating radar (GPR), dynamic cone penetrometer (DCP), portable falling weight deflectometer (PFWD), and test pit excavation were performed on an asphalt pavement. Eight test sections, about 400*m* from each other, were selected and subjected to the testing. Data obtained from the field testing were analyzed to assess the reliability and adequacy for using these testing devices and procedures to evaluate pavement layer thickness and bearing capacity. Test results and analyses indicated that GPR and DCP could both be used in estimating the pavement layer thickness. However, DCP devise could not produce reliable results for weaker layers, such as subbase and or subgrade. PFWD and DCP data were used to estimate pavement layer parameters, such as resilient modulus and had given acceptable results.

Key words: *Detection; Dynamic cone penetrometer (DCP); Ground penetrating radar (GPR);Portable falling weight deflectometer (PFWD); Thickness.*

Introduction

Coring, excavation, and sampling techniques have traditionally been used in estimating bearing capacity and thickness of roadway pavements. However, these techniques are destructive and can have significant impact on traffic. To overcome these shortcomings, many nondestructive and/or semi-destructive equipment and pavement evaluation processes have been developed, such as falling weight deflectometer (FWD), Dynamic cone penetrometer (DCP), and Ground penetrating radar (GPR).

GPR instrument is one of the commonly used techniques for estimation of pavement thickness and layer uniformity. The form of the reflection wavelength could be used in assessing the quality of pavement layer materials [1]. Lahouar and Qadi [2] used GPR technique to evaluate pavement layer thickness and concluded that compared to thickness directly measured, the average difference was small, about 2.5%. The other testing device, DCP has been widely used to evaluate stiffness/strength of aggregate base and subgrade layer of roadways. This testing device is more applicable for evaluation and analysis of soil properties. In their study, Mohammadi et al. [3] used DCP system and established good relationships among modulus of elasticity, shear modulus, and modulus of subgrade reaction.

FWD is another nondestructive testing device that has been used extensively for pavement evaluation. With FWD, impact loads are applied to pavement surface by dropping a mass to a loading plate sitting on the surface, from specified heights. Load-induced deflections are measured under the load and at different distances from the loading center. Pavement layer parameters can be estimated from the measured deflections by various backcalculation processes [4, 5]. Wu et al. [6] utilized the FWD backcalculation to evaluate flexible pavement structure with a stronger base layer. With FWD deflections, finite element method could be used to backcalculate pavement layer modulus and to assess pavement structural adequacy; and could be used as a basis for pavement maintenance [7].

However, the FWD is very heavy (with a maximal weight of about 1,000*kg*); requires time-consuming calibration; and is expensive. Because of these reasons, only limited organizations/companies own and operate FWD. In light of these issues, a German roadway organization has developed a portable falling weight deflectometer (PFWD), based on the same principles to those of FWD. This device is portable and lightweight, and does not require additional accessories. Kim et al. [8] used the PFWD to analyze pavement structures, and established a reasonable correlation between dynamic deflection modulus and bearing capacity of the base layer for roadway.

With such many advantages, however, nondestructive testing and evaluation still face one major obstacle. Because of the complex nature of the pavement structures, the variability of the analysis results can be affected by many factors [9], and large errors, as high as 60% in the deflection, have been reported. These factors include pavement depth, material properties, moisture content, temperature gradient, bearing capacity of subgrade layer, contact pressure, and traffic [10, 11].

DCP, PFWD, and GPR have all been used to evaluate the bearing capacity and/or thickness of roadway pavements. However, each system has its limitations because of its characteristics. For example, the DCP cannot adequately identify the interfaces among the pavement layers, and the accuracy of GPR can be adversely affected by blockages due to interference of reflection wave. Majority of past studies relied on coring and sampling of in situ materials for determination of soil properties. Therefore, few reports are available that provide direct comparisons of pavement layer properties estimated from the nondestructive evaluations with those measure in the field/lab directly.

[1] Assistant Professor, Department of Logistics Management, Shu-Te University, Kaohsiung County, Taiwan.
[2] Professor, Department of Civil Engineering, Feng Chia University, Taichung County, Taiwan.
[+] Corresponding Author: E-mail sheng@stu.edu.tw
Submitted June 9, 2010; Revised August 20, 2010; Accepted August 23, 2010.

Through field applications of the three testing devices, DCP, GPR, and PFWD, objectives of this study were to estimate the bearing capacity and thickness of the pavement structures; to compare the estimated parameters with measured parameters; and to identify the reliability of these testing devices and evaluation processes.

Descriptions of Testing Devices

The GPR device used in this study was supplied by GSSI Company (US, Model: SIR-3000), consisting of a mainframe, a display, antennae, and signal cables. Pavement information collected by a GPR device was then analyzed through a filtering process that transforms signal type data to layer thicknesses of the pavement structure. The radar signal filtering process included gain, stacking, deconvolution, migration, and Hilbert-transform [1]. The purpose of this process was to amplify the GPR signal and convert the interpolations, which established the relationship from distance-time to distance-depth by radar pulses.

The purpose of DCP penetration test was to establish the relationships among penetration depth, penetration number, and penetration ratio (PR), and then to estimate the interface conditions of the pavement layers and bearing capacity of the layers. In a DCP operation, a hammer was dropped from a fixed elevation to drive the cone into the pavement structure [12]. The asphalt surface layer was removed prior to the DCP testing and the tests were conducted on top of the aggregate base layer. The correlation between the accumulated penetration number and the penetration depth could be established. Generally, lower penetration number corresponds to deeper penetration depth, indicating a potentially weaker pavement layer. The inflection points on the penetration curve represented the interfaces of the pavement layers.

The PFWD used in this study was supplied by HMP company (Germany, Model: Prima 100). The load was applied to the pavement surface by dropping a mass from a specified height to a loading plate, sitting on top of the pavement surface. The maximum falling height of the mass was about 85*cm*. Deflection measured under the loading center and the applied load (in term of pressure) could be used to determine the static stiffness at the testing point using the following equation:

$$K = P / \delta_1 \quad (1)$$

where K = static stiffness of the pavement layer,
P = applied pressure, and
δ_1 = measured deflection under loading center.

Description of Test Sections and Field Testing Program

The test sections were located on a North-South, four-lane, divided existing urban roadway in Kaohsiung County, Taiwan. Total length of the roadway was about 2.2*km*. There were a total of eight test sections: Sections S1-S4 on southbound lane and Sections N1-N4 on northbound lane. Pavement structure was designed to consist of a 15-cm asphalt surface layer; a 50-cm aggregate base layer constructed in two equal lifts; a 50-cm subbase layer, also constructed in two equal lifts; and compacted subgrade. Overall layout of the eight test sections and the field-testing scheme are shown in Fig. 1. On both travel directions, test sections were about 400*m* from one another. The total width of each test section was 10-m (across the two traffic lanes), which was divided into four 2.5-m segments.

For each test section, GPR was first dragged on the pavement surface across the entire 10-m width of the section, from center of the roadway to pavement edge. GPR image collected was analyzed to determine layer thickness and assess the uniformity of the subbase and subgrade soils. The data were also used to identify test points for DCP and PFWD testing within each test section. The reflective wave signal depth of the GPR device was about 2-m with an accuracy of 10-cm.

As stated earlier, each 10-m wide test section was further divided into four 2.5-m segments. For each segment, the DCP and PFWD testing were performed at the locations identified by the GPR data. For DCP testing, the asphalt surface layer was removed and the DCP was performed from top of the aggregate base. The PFWD was applied on top of the asphalt surface layer. Test pits of the size 5*m* long, 1*m* wide, and 1*m* deep were excavated on each of the four test segments (Fig. 2) and thickness of each layer was measured (Fig. 3). Subgrade soil samples were taken and were subjected to laboratory testing for property characterization. Finally, material properties and pavement parameters estimated from GPR, DCP, and PFWD were compared with those measured at the test pits to assess the reliability of these testing devices. Fig. 4 shows comparisons of some test results.

Estimation of the Thickness of Construction Layers

Analysis of GPR Thickness Data

Fig. 5 shows a typical GPR reflection wave spectrum data interpretation, along with the estimated boundaries of the various layers. As noted in the figure, the red lines, marked as D1, D2, D3, and D4, represent the interfaces of the construction layers. From the boundary lines, uniform quality control during construction could be assessed.

Basically, each continuous signal of reflection wave can be used as an indicator in analyzing the depth and the uniformity of materials [13]. Straight line signals represent the uniform thickness and materials at this location, while distorted signals show non-uniform thickness or materials.

Moreover, recently researches studied the relationship between the frequencies of GPR and variations of the estimated thickness. The most important factors affecting the GPR data were the electrical conductivity and the dielectric constant [14]. To evaluate the influence of reflection wave frequency on the estimated thickness from GPR data, Loizos and Plati [1] used GPR frequencies of 500 and 2,000*MHz* in their study. It was observed that wave frequency had significant effects on the estimated thickness. Qadi et al. [15] pointed out that testing with various GPR frequencies would result in different evaluation results. To improve the accuracy of estimated depth and reduce the influence of reflection frequency, the frequency of antenna was set at 400*MHz* in this study, and the testing speed was kept low.

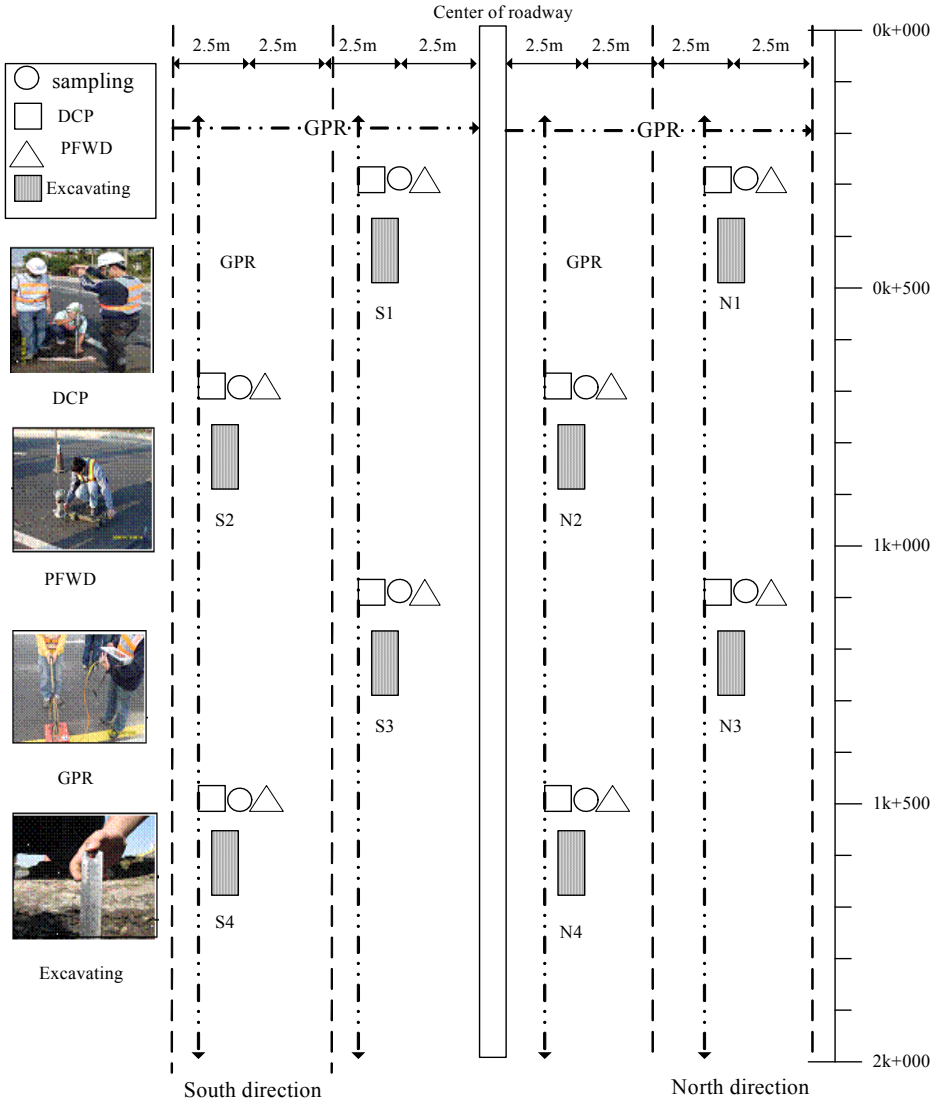

Fig. 1. Test Section Layout and Testing Schemes.

Fig. 2. Test Pit Excavation.

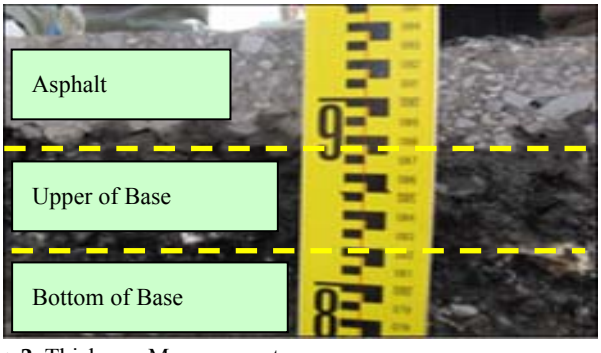

Fig. 3. Thickness Measurements**.**

As indicated in Fig. 5, thickness of each construction layer is estimated from the amplitudes of the reflected pulses collected and transformed by GPR system, at 0, 2.5, 5, 7.5, and 10*m*, along the transverse direction of the test section, starting form center of the roadway. Estimated thicknesses of the layers of the eight test sections are shown in Table 1. Please note that the precision of the GPR device is 10*cm* and the design thickness of asphalt surface layer was only 15*cm*. Therefore, the GPR device could not give reliable estimates of the asphalt layer thickness. The design pavement structure included a base thickness of 50*cm*. From Table 1, the base layer has an average thickness in the range of 45.8 to 53.1*cm*, which meets the design requirement of base thickness.

The standard deviations of thickness for base and subbase layers were 10.78 and 5.57, respectively, indicating large variations of the

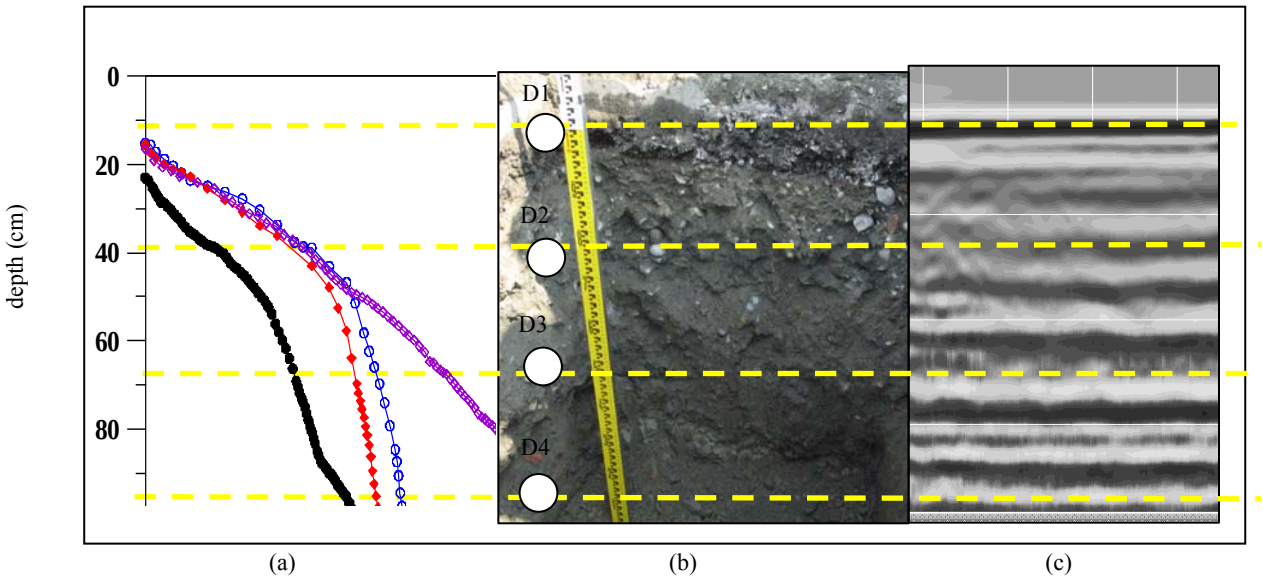

D1: Asphalt-Upper Base Interface; D2: Upper-Lower Base Interface; D3: Lower Base - Subbase Interface; D4: 30*cm* from the D3.

Fig. 4. Thickness of Each Layer Determined by Different Methods, (a) DCP, (b) Excavation and Measurement, and (c) GPR.

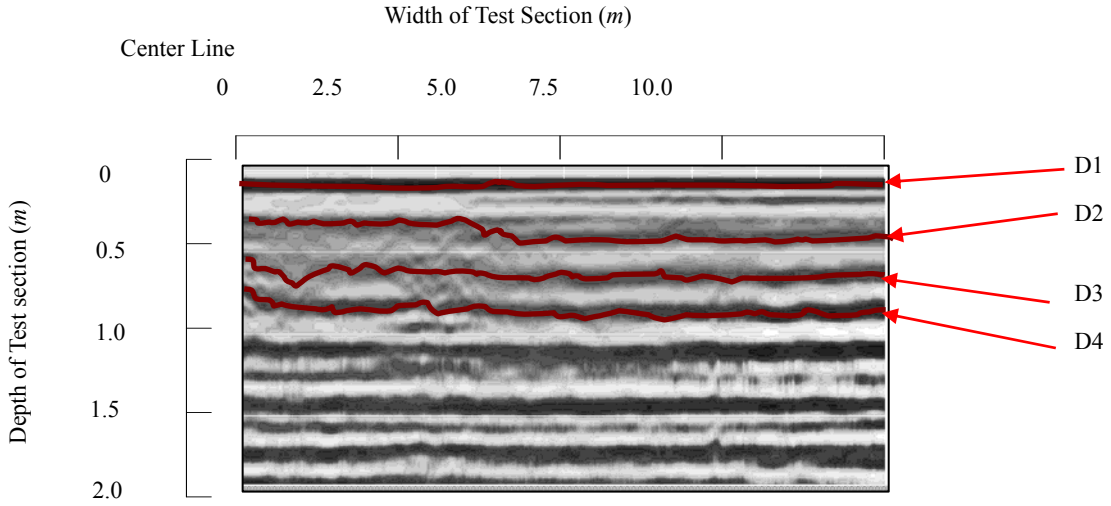

D1: Asphalt-Upper Base Interface. D2: Upper-Lower Base Interface.
D3: Lower Base - Subbase Interface. D4: Upper-Lower Subbase Interface.

Fig. 5. Distribution of GPR Detected Signal Data.

layer thickness, and in turn, poor quality control during pavement construction. Non-uniformity of thickness can also be observed in two depths, between 30 and 60*cm* from the pavement surface (within the base layer) and between 60 and 100*cm* (within the subbase layer).

Thickness Measured from Test Pits

For each segment of the eight test sections, a test pit of the size 5-m long, 1-m wide, and 1-m deep was excavated and thickness of each layer was measured. A typical plot of mean depth for various layers along the transverse direction of the test section is presented in Fig. 6. In Fig. 6, the blue solid line show the measured depths at the bottom of the bottom lift of the base layer, while the dark red line represents the depths at the top of the bottom lift of the base layer. As mentioned earlier, the design calls for the depths of the bottom lift of the base layer from 40 to 65*cm*, measured from top of asphalt surface layer. The measured values varied from 32 to 42*cm* for the top surface and from 60 to 80*cm* for the bottom surface. The variations clearly indicate a lack of quality control during construction

Also shown in Fig. 6 are depths estimated from GPR data. Same trends can be observed form the GPR data as compared with the actual measurements. Therefore, GPR evaluation can be a reliable method for quality evaluation.

It was also observed during test pit evaluation that some obstacles existed in the pavement structures, such as pipes, concrete blocks, abandoned bricks, etc., as shown in Fig. 7. These foreign materials could disturb the radar pulses and affect the signal accuracy, resulting in GPR signal fluctuation. To overcome this, GPR data were processed through a filtering process, in which, suspected signal data were removed.

Table 1. Estimated Thickness of the Structure Layer by GPR Systems.

Site	Layer Thickness (*cm*)	Distance(*m*)				
		0	2.5	5.0	7.5	10.0
S1	Base (Upper Course)	15	15	15	17	15
	Base (Bottom Course)	39	40	35	38	40
	Subbase (Upper Course)	27	25	24	22	20
	Subbase (Bottom Course)	22	18	23	19	26
S2	Base (Upper Course)	23	23	16	15	15
	Base (Bottom Course)	31	27	39	40	36
	Subbase (Upper Course)	23	24	25	18	24
	Subbase (Bottom Course)	23	23	15	25	22
S3	Base (Upper Course)	17	17	17	30	25
	Base (Bottom Course)	38	36	33	24	25
	Subbase (Upper Course)	21	20	22	16	21
	Subbase (Bottom Course)	24	27	26	30	28
S4	Base (Upper Course)	17	17	17	17	24
	Base (Bottom Course)	36	35	36	36	26
	Subbase (Upper Course)	18	20	22	22	24
	Subbase (Bottom Course)	22	22	20	24	22
N1	Base (Upper Course)	16	18	17	18	15
	Base (Bottom Course)	41	38	43	42	44
	Subbase (Upper Course)	21	21	20	17	22
	Subbase (Bottom Course)	23	23	25	26	24
N2	Base (Upper Course)	23	20	20	18	16
	Base (Bottom Course)	40	40	40	43	41
	Subbase (Upper Course)	20	17	15	12	17
	Subbase (Bottom Course)	18	21	40	37	31
N3	Base (Upper Course)	17	17	17	15	15
	Base (Bottom Course)	41	40	41	42	38
	Subbase (Upper Course)	19	36	32	38	32
	Subbase (Bottom Course)	23	10	15	19	10
N4	Base (Upper Course)	15	15	17	17	26
	Base (Bottom Course)	42	42	43	40	29
	Subbase (Upper Course)	20	19	15	16	20
	Subbase (Bottom Course)	23	25	24	27	20

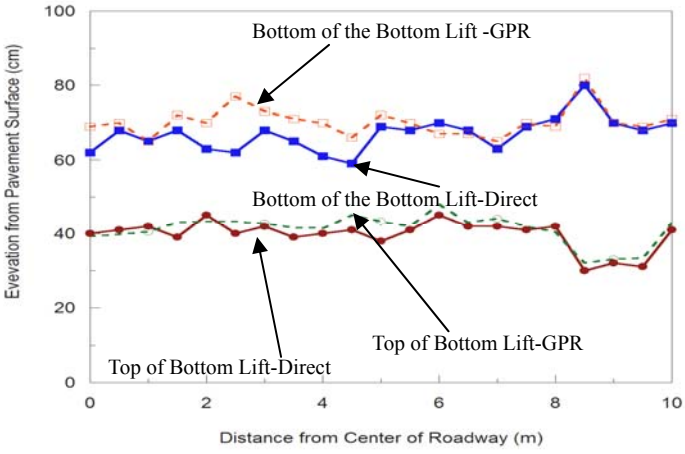

Fig. 6. A Typical Plot of Elevations of the Bottom Lift of Base Layer Measured from a Test Pit.

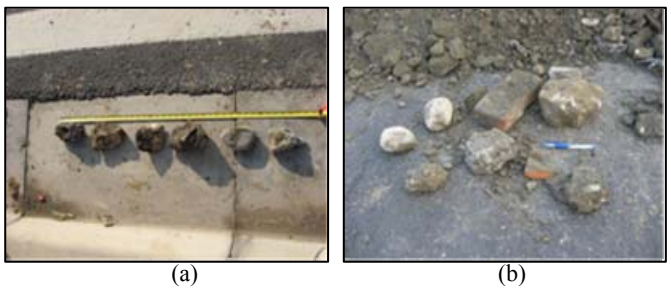

(a) (b)

Fig. 7. Obstacles Found in the Test Pits, (a) Concrete Block and (b) Abandoned Brick.

Analysis of DCP Data

Fig. 8 shows plots of DCP curves for the four test sections in the southbound direction. Please note that the 0*cm* in the vertical axis indicates the top of the aggregate base layer. Normally, the inflection points of the DCP curves represent the layer interfaces, as the dashed lines indicated. However, some of the layer boundaries could not be easily determined.

During the testing, it became apparent that the device had problems with softer layers, such as aubbase and subgrade. For soft layers, time required for penetration became much less that would

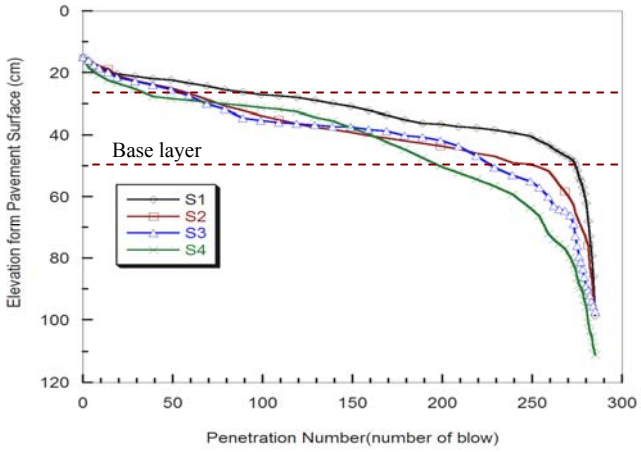

Fig. 8. DCP Penetration Curves.

not show clear inflection points. Therefore, the boundaries could not be easily observed. The errors in estimated thickness from the DCP data could be as high as 20*cm*.

Comparisons of Thickness Obtained from the GPR, DCP, and Test Pit Measurements

Both the layer thickness estimated from the GPR and DCP evaluations were compared to the data measured from the open test pits to assess the reliability of the testing procedures and analyses. The comparisons are presented in Fig. 9.

In Fig. 9(a), thickness of both base and subbase layers from all test sections were plotted against the measured data from the test pits. A linear regression analysis was also performed. As can be seen from the figure, all data clustered close to the line of equality, indicating that the data obtained from these two methods are very close. The high coefficient of determination, R^2, of 0.99 further confirms this observation.

Comparison of estimated thickness data from the DCP evaluation and the values measured from the test pits are shown in Fig. 9(b). Please note that, since the DCP method could not adequately identify boundaries of soft layer, no data from the subbase layer was included in this figure. A decent relationship between thickness estimated from the DCP data and those measured from test pits was also realized, with a coefficient of determination, R^2, of 0.91. However, obstacles, such as stone and pipeline, encountered during DCP penetration testing, would mostly cause some errors. Errors could be as high as 20*cm*.

From the analyses conducted in this section, both GPR and DCP can be used for estimation of pavement layer thickness; however, errors were higher for data collected using DCP.

Evaluation of Bearing Capacity of Pavement Structure

Laboratory Testing of Base and Subbase Materials Obtained from Test Pits

Samples of base and subbase materials were also obtained from test pits and were subjected to laboratory testing for material characterizations. Subbase materials were taken at about 30*cm* more below subbase/base interface. Properties of the subbase and base materials are listed in Tables 2 and 3, respectively.

The subbase soil was classified as A-4 to A-6 type, i.e., fine clay. The roadway was located in an area with high groundwater level. Due to its high water content, it is difficult to remove the groundwater from soil layer, which could result in low bearing capacity. AASHTO T180 specification stipulates a minimum relative compaction of subbase soils of 95% of the maximum dry density. From Table 2, the relative compaction measured ranged from 81 to 89%, which are all below the specified requirement. Please also note that the actual depths, where the samples were obtained, also varied, from 66 to 105*cm* (measured from top of the asphalt layer). This was done to avoid obstructions from obstacles and also to assess if the compaction was performed uniformly. No trend could really be observed.

Table 3 shows the properties of materials of base layer at eight test sites. All relative compaction are greater than the specified requirement of 95%, which indicates excellent quality of construction for base layer. In addition, California bearing ratio (CBR) values are commonly used as indicator of strength and bearing

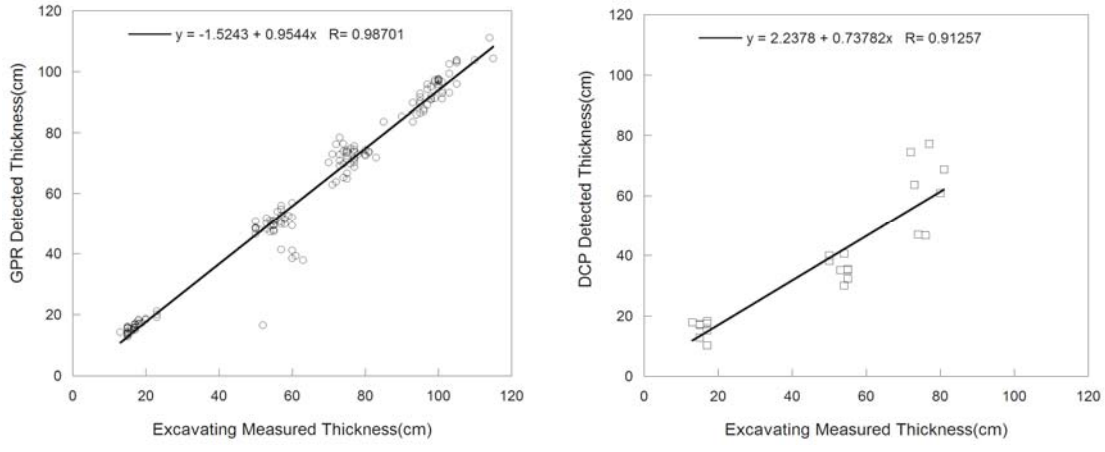

(a) (b)

Fig. 9. Comparisons of Layer Thickness Obtained from GPR, DCP, and Test Pit Measurements, (a) GPR vs. Test Pit Measurements and (b) DCP vs. Excavation Measurements.

Table 2. Material Properties of Subbase Layer.

Items / Site	N1	N2	N3	N4	S1	S2	S3	S4
Sampling Depth (*cm*)	85	102	105	80	83	66	80	101
Moisture Content (%)	23.8	25.1	24.4	21.6	20.2	18.5	16.2	14.0
Wet Density (g/cm^3)	1.82	1.92	1.96	1.79	1.80	1.74	1.87	1.53
Dry Density (g/cm^3)	1.56	1.48	1.57	1.49	1.50	1.54	1.58	1.64
Maximum Dry Density (g/cm^3)	1.87	1.78	1.82	1.83	1.81	1.86	1.82	1.84
Relative Compaction (%)	83	83	86	81	83	83	87	89
O.M.C. (%)	15.6	15.3	13.6	16.0	15.0	15.1	13.9	13.6
Wetted CBR (%)	10.8	11.1	10.4	10.8	14.7	15.2	14.6	10.8

Table 3. Material Properties of Base Layer.

Items / Site	N1	N2	N3	N4	S1	S2	S3	S4	Specification
Soil Depth (*cm*)	35	38	41	46	35	36	38	35	-
Abrasion (%)	34	33	30	31	34	26	28	26	<50
Maximum Dry Density (g/cm^3)	1.85	1.87	2.0	1.92	1.83	1.88	1.83	1.84	-
Relative Compaction (%)	96	96	81	100	100	96	91	94	>95
O.M.C. (%)	10.8	11.6	11.6	10.0	10.0	10.5	13.2	14.3	-
Wetted CBR (%)	63	65	60	61	56	60	60	63	>80

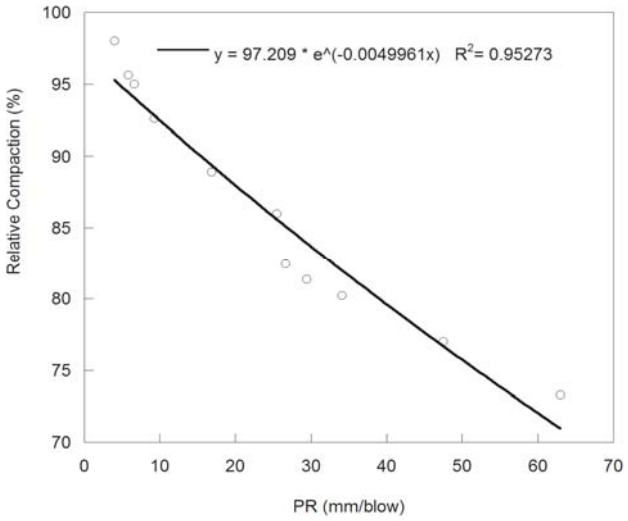

Fig. 10. Relative Compaction vs. PR.

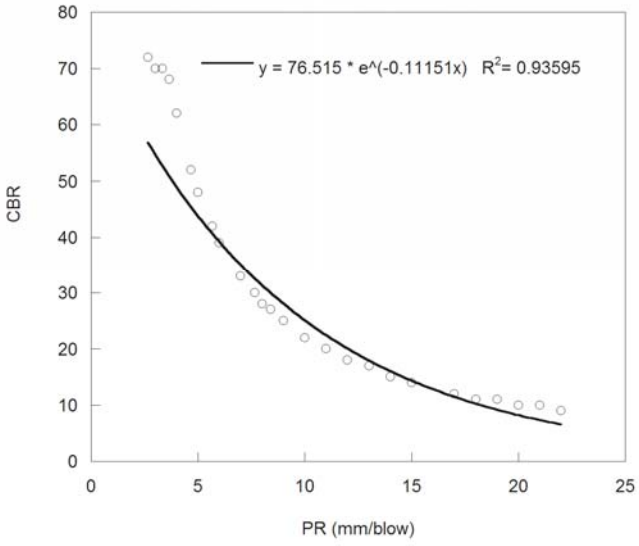

Fig. 11. CBR vs. PR.

capacity of a subgrade, subbase, and base course material for use in roadway [16]. Optimum moisture content (OMC) values are indicator of the water content of optimum compaction capacity. The CBR and OMC values for the base layers are from 56 to 63%, and 10 to 14%, respectively.

Analysis of DCP Penetration Data

In this study, the DCP penetration curves were used to estimate layer thickness as well as to assess bearing capacity of structure layers. As discussed in earlier sections of the paper, the inflection points of the penetration curves represented the boundaries of the pavement layers. Penetration Ratio (PR), defined as the depth of penetration caused by a single blow of the DCP mass, could be used to evaluate the density and hardness of construction materials [17].

The PR data obtained from the test sections by the DCP device were correlated to the relative compactions (RC) measured from the test pits (described in previous section) and the CBR data, as presented in Figs. 10 and 11, respectively. Regression analyses were also performed to develop the correlations between RC and PR and between CBR and PR. Decent relationships were developed between these two parameters, with a coefficient of determination R^2 of 0.95 and 0.94.

From Fig. 10, it is observed that a higher PR value corresponds to a lower relative compaction for the pavement layers. The specified relative compaction of 95% corresponds to a PR value of about 5. Similarly, in Fig. 11, the CBR value decreases as the PR value increases. The Asphalt Institute (AI) specification MS-1 requires that CBR values need to be above 80%, which are corresponded to a PR value of about 3.

As presented by Webster et al. [18], from the DCP data analysis equations, the layer modulus of elasticity (Mr) could be estimated. In this study, moduli of elasticity of the base layer and subbase layer materials for the eight test sections were estimated, as presented in Table 4.

Table 4. Base and Subbase Layer Modulus of Elasticity Estimated from PR.

Site	Base Layer		Subbase Layer	
	PR (*mm*/blow)	Mr (kg/cm^2)	PR (*mm*/blow)	Mr (kg/cm^2)
S1	5.89	33	12.09	21
S2	3.47	45	12.65	19
S3	4.61	51	11.47	21
S4	3.99	43	14.01	15
N1	6.16	29	18.79	13
N2	3.17	47	23.43	10
N3	2.41	74	26.01	8
N4	1.57	78	25.04	9

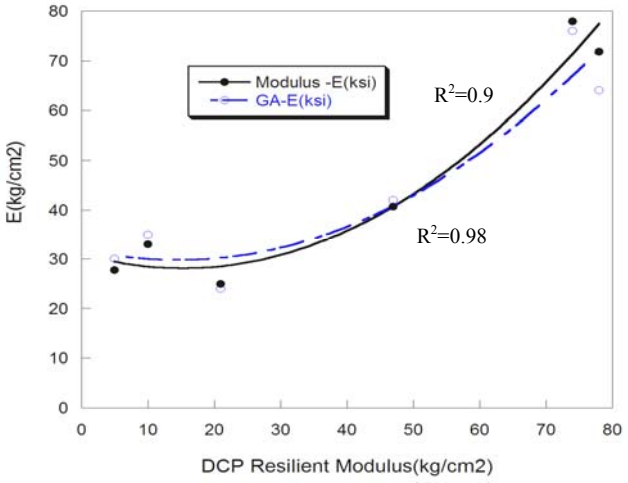

Fig. 12. Relationships between E Values Obtained from PFWD BackCalculated and from DCP Data.

Roadway Bearing Capacity and Deflections Backcalculation

In the PFWD tests, load was applied to a loading plate, sitting on top of the pavement surface, by dropping a mass of 10-kg from fixed heights. Deflections under the loading center and at two other locations, 30 and 60*cm* from the loading center were measured. The measured deflections were then analyzed using two established procedures to backcalculte the pavement layer parameters. To minimize obstruction to the traffic of this heavily utilized roadway, PFWD tests were only performed Test Sections S4, N3, and N4.

From the deflection measured under the loading center, the pavement static stiffness at that point can be calculated as $K = P/\delta_1$. The resilient modulus (Mr_{PFWD}) of the pavement layers were backcalculated from PFWD deflection data based on the Boussinesq theory: calculation should take into consideration of disk radius (r), Poisson's ratio (v), material's coefficient (η) and static stiffness. The Mr_{PFWD} value can be expressed according to the Boussinesq theory [19]:

$$Mr_{PFWD} = \frac{\eta(1-\nu^2)P \cdot r}{\delta_1} \quad (2)$$

Where,

Table 5. Calculation Results of Testing Deflection Modulus and GA Resilient Modulus.

Test Section	Vertical Depth(*cm*)	Construction Layer	Boussinesq Mr_{PFWD} (kg/cm^3)	DCP Resilient Modulus (kg/cm^3)
S4	0	Asphalt	185	N/A
S4	16	Base	53	77
S4	90	Subbase	7	5
N4	0	Asphalt	137	N/A
N4	16	Base	21	46
N4	90	Subbase	16	21
N3	0	Asphalt	161	N/A
N3	65	Subbase	16	10

η = Material coefficient (= $\pi/2$ for rigid pavement and 2 for flexible pavement),
δ_1 = Measured deflection under the loading center (μm),
P = Loaing pressure (Pa),
r = Radius of the loading plate (m), and
v = Poisson's ratio.

Since a pavement is a multi-layer system, deflections measured at the other two locations were also needed, as shown below:

$$Mr_{2,3} = \frac{(1-\nu^2)\, r^2 \cdot P}{\delta_{2,3} \cdot l} \quad (3)$$

Where,
$Mr_{2,3}$ = Moduli of elasticity estimated using deflections measured at the locations 30 and 60*cm* from the loading center,
$\delta_{2,3}$ = Measured deflections at the locations 30 and 60*cm* from the loading center (μm).

A genetic algorithm (GA) program, developed by Lee [20], was also used to backcalculate the layer parameters using the PFWD measured deflections. Modulus of elasticity for the test pavements estimated by the above mentioned two procedures were compared with each other and to those determined from the DCP procedure (see Tables 5 and 6).

From Table 5, it is observed that the differences between the modulus values backcalculated from the PFWD deflections using the Boussinesq theory and those obtained from the DCP data range from 24 to 60%. These differences could be resulted from the assumption of semi-infinitive boundaries by the Boussinesq theory. However, these differences are consistent with values presented in literatures, and are considered acceptable.

Table 6 presents E values estimated from three methods. It is observed that E values backcalcultaed from the PFWD deflection data using the Boussinesq theory and the GA program are relative close. For base layers, values obtained from three procedures seem to be close; however, for subbase layers, values determined from the DCP testing are greatly different from those estimated from the other two methods. One possible reason for the discrepancies is the light load used in the PFWD testing that can not produce enough deflections to be used for estimation of the subbase layer.

Correlations of the PFWD deflection based modulus of elasticity values were also plotted against those developed from the DCP data, as shown in Fig. 12. Decent relationships existed, represented by the R^2 values above 0.90 for both cases.

Table 6. Comparison of the Boussinesq Dynamic Resilient Modulus from PFWD and the DCP Resilient Modulus.

Test Section	E value from Modulus (kg/cm^2)			E value from GA (kg/cm^2)			E value from DCP Data (kg/cm^2)	
	Asphalt	Base	Subbase	Asphalt	Base	Subbase	Base	Subbase
S4	488	77	32	488	75	34	73	10
N4	931	71	27	1033	63	29	77	5
N3	734	40	25	740	41	24	46	21

Conclusions

From the study, the following conclusions are derived:

1. The GPR device can be an effective testing device in determining pavement layer thickness.
2. The DCP testing is appropriate for estimation of stronger layers; such as the base layer; for weak layers, such as subbase, the DCP is not adequate in delineating the layer boundaries.
3. The PFWD testing device can be an effective device in backcalculating pavement layer parameters. The predicted values closely approximated to the values obtained from DCP data evaluation. Accordingly, the bearing capacity of roadway can be reasonably predicted by these testing devices.
4. The evaluation on soft region of roadway requires sampling at deeper depth, such as from the subbase/subgrade layers.

Acknowledgments

The authors gratefully acknowledge advisory support from the Professor Deng-Fong Lin, I-Shou University, and financial support from the Technology Construction and Planning Agency, Ministry of the Interior in Taiwan.

References

1. Loizos, A. and Plati, C., (2007). Accuracy of Pavement Thicknesses Estimation Using Different Ground Penetrating Radar Analysis Approaches, *NDT & E International*, 40(2), pp. 147-157.
2. Lahouar, S. and Qadi, I.L., (2008). Automatic Detection of Multiple Pavement Layers from GPR Data, *NDT & E International*, 41(2), pp. 69-81.
3. Mohammad, S.D., Nikoudel, M.R., Rahimi, H., and Khamehchiyan, M.,（2008）. Application of the Dynamic Cone Penetrometer (DCP) for Determination of the Engineering Parameters of Sandy Soils, *Engineering Geology*, 101(3-4), pp. 195-203.
4. Seo, J.W., Kim, S.I., Choi, J.S., and Park, D.W., (2009). Evaluation of Layer Properties of Flexible Pavement Using a Pseudo-Static Analysis Procedure of Falling Weight Deflectometer, *Construction and Building Materials*, 23(10), pp. 3206-3213.
5. Tholen, O., Sharma, J., and Terral, R.L., (1985). Comparison of Falling Weight Deflectometer with Other Deflection Testing Devices, *Transportation Research Record*, No. 1007, pp. 131-144.
6. Wu, Z., Chen, X., Mohammad, L.N., and Zhang, Z., (2009). Field Structural Performance of Stabilized Blended Calcium Sulfate (BCS) Materials under Accelerated Pavement Testing, *International Journal of Pavement Research and Technology*, 2(3), pp. 98-105.
7. Picoux, B., Ayadi, A.E., and Petit, C., (2009). Dynamic Response of a Flexible Pavement Submitted by Impulsive Loading, *Soil Dynamics and Earthquake Engineering*, 29(5), pp. 845-854.
8. Kim, J.R., Kang, H.B., Kim, D., Park, D.S., and Kim, W.J., (2007). Evaluation of in Situ Modulus of Compacted Subgrades using Portable Falling Weight Deflectometer and Plate-Bearing Load Test, *Journal of Materials in Civil Engineering*, 19(6), pp. 492-499.
9. Lin, Y.Y., Chang, C.F., and Lee, W.T., (2008). Effects of Thickness on the Largely-Deformed JKR (Johnson–Kendall–Roberts) Test of Soft Elastic Layers, *International Journal of Solids and Structures*, 45(7-8), pp. 2220-2232.
10. Long Term Pavement Performance (LTPP), (2000). *LTPP Manual for Falling Weight Deflectometer Measurings Operational Field Guidelines*, Version 3.1, Long-Term Pavement Performance Team, Federal Highway Administration, McLean, Virginia, USA.
11. Rushing, T.S. and Tingle, J.S., (2009). Full-Scale Evaluation of Mat Surfacings for Roads Over Sand Subgrades, *Journal of Terramechanics*, 46(2), pp. 57-63.
12. Newcomb, D.E., Chabourn, B.A., Deusen, D.A.V., and Burnham, T.R., (1995). Initial Characterization of Subgrade Soils and Granular Base Materials at the Minnesota Road Research Project, *Report No. MN/RC-96/19*, Minnesota Department of Transportation, Minnesota, USA.
13. Kadioglu, S., (2008). Photographing Layer Thicknesses and Discontinuities in a Marble Quarry with 3D GPR Visualization, *Journal of Applied Geophysics*, 64(3-4), pp. 109-114.
14. Saarakento, T., (1997). Using Ground Penetrating Radar and Dielectric Probe Measurements in Pavement Density Quality Control, *Transportation Research Record*, No. 1575, pp. 34-41.
15. Qadi, I.L., Xie, W., and Roberts, R., (2008). Scattering Analysis of Ground-penetrating Radar Data to Quantify Railroad Ballast Contamination, *NDT & E International*, 41(6), pp. 441-447.
16. Hazirbaba, K. and Gullu, H., (2010). California Bearing Ratio Improvement and Freeze-Thaw Performance of Fine-Grained Soils Treated with Geofiber and Synthetic Fluid, *Cold Regions Science and Technology*, 63(1-2), pp.50-60.
17. Tom, B. and Dave, J., (1993). In Situ Foundation Characterization Using The Dynamic Cone Penetrometer, Final Report No. 9PR3001, Minnesota Department of Transportation Office of Research Administration, Minnesota ,USA.
18. Webster, S.L., Brown, R.W., and Porter, J.R., (1994). Force Projection Site Evaluation Using the Electric Cone Penetrometer and the Dynamic Cone Penetrometer, *Technical Report, GL-94-17*, U.S. Waterways Experimental Station, USA.

19. Seyman, E., (2003). Use of Portable Falling Weight Deflectometer, Dynamic Cone Penetrometer and Humboldt Geogauge for Quality Assessment During Road Formation and Foundation Construction, *Master Thesis*, Department of Science in Civil Engineering, Louisiana State University, Louisiana, USA.
20. Lee, Y.C., (1997). Condition Assessment of Flexible Pavements Using FWD Deflections, *PhD Dissertation*, North Carolina State University, Raleigh, North Carolina, USA.